

Dynamics of NF- κ B and I κ B α Studied with Green Fluorescent Protein (GFP) Fusion Proteins

INVESTIGATION OF GFP-p65 BINDING TO DNA BY FLUORESCENCE RESONANCE ENERGY TRANSFER*

Received for publication, January 13, 2000, and in revised form, February 29, 2000
Published, JBC Papers in Press, March 15, 2000, DOI 10.1074/jbc.M000291200

Johannes A. Schmid^{‡§}, Andreas Birbach[‡], Renate Hofer-Warbinek[‡], Margarete Pengg[‡],
Ursula Burner[¶], Paul G. Furtmüller[¶], Bernd R. Binder[‡], and Rainer de Martin[‡]

From the [‡]Department of Vascular Biology and Thrombosis Research, University of Vienna, Vienna A-1235, Austria and the [¶]Department of Biochemistry, Institute of Chemistry, University of Agricultural Sciences, Vienna A-1190, Austria

We investigated the dynamics of nuclear transcription factor κ B (NF- κ B) by using fusion proteins of the p65 subunit with mutants of green fluorescent protein (GFP). GFP-NF- κ B chimeras were functional both *in vitro* and *in vivo*, as demonstrated by electrophoretic mobility shift assays and reporter gene studies. GFP-p65 was regulated by I κ B α similar to wild type p65 and associated with its inhibitor even if both proteins were linked to a GFP protein. This finding was also verified by fluorescence resonance energy transfer (FRET) microscopy and studies showing mutual regulation of the intracellular localization of both GFP chimeras. Incubation of GFP-p65 with fluorescently labeled NF- κ B-binding oligonucleotides also resulted in FRET. This effect was DNA sequence-specific and exhibited saturation characteristics. Application of stopped-flow fluorometry to measure the kinetics of FRET between GFP-p65 and oligonucleotides revealed a fast increase of acceptor fluorescence with a plateau after about 10 ms. The observed initial binding rate showed a temperature-dependent linear correlation with the oligonucleotide concentration. The association constant calculated according to pre-steady state kinetics was $3 \times 10^6 \text{ M}^{-1}$, although equilibrium binding studies implied significantly higher values. This observation suggests that the binding process involves a rapid association with a rather high off-rate followed by a conformational change resulting in an increase of the association constant.

Nuclear factor κ B (NF- κ B)¹ or Rel proteins are members of a family of eukaryotic transcription factors, which share structural and functional similarities. They are characterized by the presence of a so called Rel homology domain, RHD, with a length of about 300 amino acids. Their active DNA-binding

forms are homodimeric or heterodimeric complexes consisting of combinations of members of this protein family.

Their common structural feature, the RHD, is important for dimerization, DNA binding, and regulatory binding to inhibitory molecules of the I κ B family (for review see Refs. 1–3). The NF- κ B/Rel factors can be divided into different functional classes. The most important distinction is the presence of transactivating domains in the p65 (RelA), RelB, c-Rel, and v-Rel subunits, which are not contained in the p50 and p52 subunits. The latter Rel family members originate from p100 and p105 precursors, respectively, by proteolytic cleavage of an inhibitory, I κ B-like sequence from the proform. In most cells, NF- κ B complexes are normally localized to the cytosol as inactive complexes with inhibitory I κ B proteins. However, at least in certain cell types mainly of the hematopoietic cell lineage, particular NF- κ B members are constitutive in the nucleus, where they have essential roles in cellular proliferation and differentiation (2).

The most abundant NF- κ B dimers, p50/p65 and p65/p65, which are important for the inducible expression of genes involved in inflammation, are maintained in the cytosol as inactive complexes with I κ B proteins (I κ B α , I κ B β , and I κ B ϵ), which mask their nuclear localization sequence by binding to the RHD (2, 4, 5). In these cases, the activation of NF- κ B is tightly regulated by signal transduction pathways leading to the phosphorylation, ubiquitinylation, and proteasomal degradation of I κ B molecules (for review see Ref. 6). It is generally assumed that binding of different signaling molecules such as TNF α to the corresponding receptors on the cell surface leads to an oligomerization of receptors (7) and cytosolic adapter molecules (such as the TNF receptor-associated factors, TRAFs), followed by activation of downstream kinases such as NIK (NF- κ B-inducing kinase) or MEKK1 (MAPK/ERK kinase kinase-1) (8–10). These kinases phosphorylate and activate so-called I κ B kinases (IKK1/IKK- α and IKK2/IKK- β), which are part of a multiprotein complex termed the signalosome that is responsible for signal-induced phosphorylation of I κ B molecules on two Ser residues that are close together in the N-terminal regulatory domain (11–15). This phosphorylation triggers the ubiquitinylation of I κ B by β -TrCP variants (16, 17) and its degradation by proteasomes. The proteolytic elimination of I κ B molecules leads to the release of NF- κ B and the unmasking of its nuclear localization sequence, which is followed by translocation to the nucleus and binding to cognate DNA sequences.

The occurrence of different NF- κ B dimer isoforms, the formation of complexes with distinct I κ B molecules, which exhibit diverse phosphorylation and degradation characteristics (2, 18), and modifications in the signaling cascades leading to release of NF- κ B provide enormous variation for the activation

* This study was supported by a grant from the Austrian Science Foundation (SFB5-12). The costs of publication of this article were defrayed in part by the payment of page charges. This article must therefore be hereby marked "advertisement" in accordance with 18 U.S.C. Section 1734 solely to indicate this fact.

§ To whom correspondence should be addressed: Dept. of Vascular Biology and Thrombosis Research, University of Vienna, Brunnerstr. 59, A-1235 Vienna, Austria. Tel.: 43-1-86634-471; Fax: 43-1-86634-623; E-mail: johannes.schmid@univie.ac.at.

¹ The abbreviations used are: NF- κ B, nuclear factor κ B; GFP, green fluorescent protein; CHO, Chinese hamster ovary cells; FRET, fluorescence resonance energy transfer; GFP, green fluorescent protein; HEX, hexachlorocarboxyfluorescein; HUVEC, human umbilical vein endothelial cells; I κ B, inhibitor of κ B; RHD, Rel homology domain; TET, tetra-chlorocarboxyfluorescein; TNF α , tumor necrosis factor α ; β -TrCP, β -transducin repeat-containing protein; YFP, yellow fluorescent protein.

of NF- κ B. Moreover, it has been shown that different members of the NF- κ B family bind slightly distinct DNA sequences with different affinities (19), which represents an additional level of transcriptional regulation of NF- κ B-dependent genes. The classical NF- κ B consensus sequence, 5'-GGGRNNYYCC-3' (R indicates purine, and Y is pyrimidine), is an imperfect palindrome, which in itself allows a rather high level of variation (2). Interestingly, the p65/p65 homodimer can bind to just one half-site of the target sequence, thereby expanding the number of potential NF- κ B-regulated genes dramatically. Differences in the second half-site lead to variations in the association constants (20).

Up to now, the binding of NF- κ B to its cognate DNA sequence was studied mainly by electrophoretic mobility shift assays, which allows only an equilibrium binding analysis. Using this technique, a rather slow binding of NF- κ B to DNA was reported, with a plateau after about 60 min in the presence of poly(dI-dC) (21) or within approximately 5 min in the absence of an excess of unspecific competitor DNA (22). However, the high DNA-binding affinity of NF- κ B complexes, with association constants in the range of 10^{10} to 10^{13} M $^{-1}$ (19, 23, 24), would argue for much faster binding kinetics, which cannot be resolved by the electrophoretic mobility shift techniques used so far. Therefore, we generated a GFP-NF- κ B fusion protein suited for the investigation of not only the dynamics of this transcription factor in living cells but also the binding to DNA *in vitro*, by applying the principle of FRET. This principle is based on the fact that energy transfer occurs between two fluorophores when they are in close proximity (<10 nm), and the emission spectrum of the first fluorophore (the donor) overlaps with the excitation spectrum of the second (the acceptor). The energy transfer is dependent on the quantum yield of the donor, the degree of spectral overlap, and the orientation of the fluorophores, and it declines with the sixth power of the distance. A close association of two suited fluorophores and excitation of the donor results in an increase of acceptor fluorescence and/or a decrease in donor fluorescence due to FRET (25–27). By applying this phenomenon, we could measure the kinetics of the interaction between GFP-NF- κ B and fluorescently labeled oligonucleotides using stopped-flow fluorometry. We found a rapid association, reaching a plateau within about 10 ms, and a subsequent slow decrease of the energy transfer. This phenomenon, as well as the difference between association constants calculated from initial binding rates and those derived from equilibrium binding studies, indicates that the rapid association is followed by a conformational change of the NF- κ B-DNA complex, which increases the affinity.

The technique that we describe should open a wide field of possible applications, for instance the investigation of the interaction between various NF- κ B family members and different DNA sequences for drug screening of potential inhibitors. Moreover, it could be very valuable for the analysis of the dynamics and biochemical characteristics of protein-protein interactions in solution using CFP and YFP fusion proteins. In that respect, it should have considerable advantages over conventional assays of macromolecular interactions, which usually do not reflect the dynamics of the association, and also over kinetics-based methods using proteins immobilized on chip surfaces (such as surface plasmon resonance on BIAcoreTM chips), which do not represent the behavior of macromolecules in solution.

MATERIALS AND METHODS

Construction of GFP-NF- κ B and CFP-I κ B α Variants—The p65 subunit of NF- κ B was amplified by PCR with *Pfu* DNA polymerase using the sequences 5'-AAA AAA GCT TCC ACC ATG GAC GAA CTG TTC C-3' and 5'-AAA AGG ATC CAA GGA GCT GAT CTG ACT CAG-3' for forward and reverse primers, respectively. The PCR fragment was

cloned in frame into the *Bam*HI and *Hind*III sites of pEGFP-C1 (CLONTECH Laboratories Inc., Palo Alto, CA), generating a fusion protein of the mammalian codon-optimized enhanced GFP protein with p65 linked to its C terminus. A YFP-p65 construct was generated in the same way using pEYFP-C1 (CLONTECH). The CFP-I κ B α construct (with CFP linked to the N terminus of I κ B) was designed by transferring the coding region of I κ B from the construct described previously (28) into the pECFP-C1 plasmid (CLONTECH). An I κ B-CFP construct, in which the CFP tag is linked to the C terminus of I κ B, was cloned by inserting a PCR fragment without a stop codon into the *Nhe*I site of the pECFP-C1 vector. All constructs were verified by restriction and sequence analysis.

Cell Culture and Transfections—CHO cells were cultured in MEM- α medium (Life Technologies, Inc.) and 293 and HeLa cells in Dulbecco's modified Eagle's medium (Life Technologies, Inc.), both including 10% fetal calf serum and 2 mM glutamine. HUVEC were grown as described (29). Transient transfections were performed with the LipofectAMINE PlusTM system (Life Technologies, Inc.) according to the manufacturer's protocol. In brief, CHO cells (one well of a six-well plate, 10 cm²) were transfected with 1 μ g of DNA, 5 μ l of Plus reagent, and 2 μ l of LipofectAMINE for 3.5 h and 293 cells with 1 μ g of DNA, 4 μ l of Plus reagent, and 3 μ l of LipofectAMINE for 4 h. HeLa cells were transfected with 1.5 μ g of DNA, 5 μ l of Plus reagent, and 4 μ l of LipofectAMINE for 5 h and HUVEC with 1.5 μ g of DNA, 8 μ l of Plus reagent, and 4 μ l of LipofectAMINE for 2.5 h. Stable transfection of CHO cells with GFP-p65 was performed with the construct after linearization by *Mlu*I together with a puromycin resistance vector (pPUR, CLONTECH, linearized by *Eco*RI) using the LipofectAMINE protocol as described above. Selection was performed with 50 μ g/ml puromycin (CLONTECH), and single GFP-p65-expressing clones were generated by limiting dilution and evaluation of the fluorescence.

Electrophoretic Mobility Shift Assays—Whole cell extracts from GFP-p65 expressing CHO cells were prepared by repeated freeze-thawing in buffer A (20 mM Tris/HCl, pH 7.9, 1 mM EDTA, 5 mM MgCl₂, 50 mM KCl, 1 mM dithiothreitol) and pelleting of cell debris at 14,000 \times g for 30 min. Labeling of double-stranded NF- κ B-binding oligonucleotides and electrophoretic mobility shift assays were done as described (30). Imaging and quantification of protein-bound and free oligonucleotides were done with PhosphorImager equipment (Molecular Dynamics).

Reporter Gene Assays—293 or HeLa cells were transiently transfected with a luciferase reporter construct under the control of the NF- κ B-dependent I κ B promoter (28) and a β -galactosidase vector containing a ubiquitin promoter (pUB6/V5-His/*lacZ*, Invitrogen, Groningen, Netherlands) as internal control. GFP variants of p65 or I κ B α , wild type p65 (31) or I κ B α (28), were co-transfected with reporter and control vectors using LipofectAMINE Plus as described. Cell extracts were prepared by repeated freeze thawing in 0.1 M potassium phosphate buffer (pH 7.8). Luciferase activity was determined as described (32) and normalized to β -galactosidase activity determined with chlorophenol red- β -D-galactopyranoside as substrate and colorimetric detection at 570 nm.

Morphological Studies and FRET Imaging—HUVEC or HeLa cells were transiently transfected with YFP-p65, CFP-I κ B, or both and investigated 1 day after transfection on a Nikon Diaphot TMD microscope using filter sets, which discriminate between CFP and YFP fluorescence (Omega Optical Inc., Brattleboro, VT) and a cooled charge-coupled device camera (Kappa GmbH, Gleichen, Germany). For FRET microscopy studies, images were taken with the donor filter set (for CFP) and an acceptor filter set (XF88, Omega Optical Inc.) with excitation of the donor (440 nm), a 455 nm dichroic mirror, and an emission filter for the acceptor (535 nm). Images were captured with both filter sets under identical conditions for control cells transfected with CFP and YFP and cells transfected with I κ B-CFP and YFP-p65. Ratio images were calculated by dividing the acceptor filter image by the donor image (33) using NIH image software, version 1.62. Nuclear import of GFP-p65 after the addition of TNF α (200 international units/ml) to HUVEC was investigated by time series imaging using confocal laser scanning microscopy on MRC600 equipment (Bio-Rad).

Scanning and Stopped-flow Fluorometry—Extracts containing GFP-p65 were prepared from stable CHO transfectants as they were for electrophoretic mobility shift assays by repeated freeze-thawing in buffer A, centrifugation at 100,000 \times g for 1 h at 4 $^{\circ}$ C, and filtration of the supernatant through a 0.45- μ m filter. GFP-p65 extracts were incubated in buffer A with TET- or HEX-labeled double-stranded oligonucleotides comprising the NF- κ B binding site of the I κ B α promoter (plus strand, 5'-CTT GGA AAT TCC CCG-3'; minus strand, 5'-TCG GGG AAT TTC CAA-3'; with both labeled on the 5'-end). The competitor oligonucleotide had the same sequence but without label. The mutant

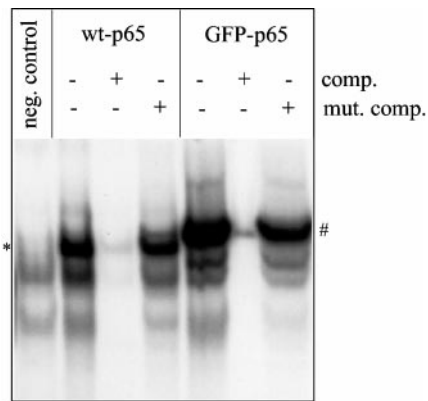


FIG. 1. Binding of GFP-p65 to its cognate DNA sequence. Extracts from CHO cells that were transiently transfected with wild type p65 (*wt-p65*) or GFP-p65 were subjected to electrophoretic mobility shift assays with 32 P-labeled NF- κ B-binding oligonucleotides in the absence (-) or presence (+) of a 200-fold molar excess of unlabeled competitor oligonucleotides of the same DNA sequence (*comp.*) or a mutated sequence (*mut. comp.*). The localizations of wild type p65 (*) and GFP-p65 (#) are indicated.

oligonucleotide had the sequence 5'-TTA GAT TTT ACT TTC CGA GA-3' with a 5'-TET-label and the corresponding complementary strand. Emission scans were performed on a JASCO FP-920 spectrofluorometer with excitation at 482 nm (bandwidth, 18 nm) and an emission bandwidth of 10 nm. Stopped-flow fluorometry was performed with SX-18MV equipment (Applied Photophysics, Leatherhead, Surrey, UK) at 15 °C or 37 °C with excitation at 490 nm and a 530-nm long pass emission filter. In total, 100 μ l were shot into a flow cell with a 1-cm light path. For monitoring the initial binding phase, fluorescence was recorded for 50 ms with 2000–4000 data points, and the recorded time course of fluorescence was fitted with an algorithm for a single exponential reaction. On- and off-rates were calculated from the concentration dependence of the initial binding rates observed (with k_{on} given by the slope of the linear curve fit and k_{off} by the intercept on the y axis (34)). The association constant of the initial binding phase is defined as k_{on}/k_{off} . Investigation of longer time periods was done using 2000 data points for the initial 50 ms and 2000 data sets for subsequent 1000 ms.

RESULTS

Functional Integrity of GFP-p65-NF- κ B—We generated a fusion construct of the p65 NF- κ B protein with a mammalian codon-optimized enhanced mutant of GFP linked to the N terminus of p65. On the basis of the crystal structure of the p65 homodimer (20) or the p50/p65 heterodimer (35) bound to a cognate DNA sequence, we expected that the N-terminal GFP tag would not interfere with binding of p65 to DNA. Moreover, the C terminus comprising the two transactivation domains, which are essential for interaction with the transcriptional machinery, should remain unaffected by the N-terminal GFP. The C-terminal domain was also reported to be the target of a phosphorylation event that is essential for full transcriptional activity (36). To determine whether the GFP-p65 fusion protein is still functional with respect to binding *in vitro*, we performed electrophoretic mobility shift assays with the fusion protein compared with wild type p65. CHO cells were transiently transfected with equal amounts of wild type p65 or GFP-p65, and extracts were prepared as described under “Materials and Methods.” Incubation of these extracts with 32 P-labeled NF- κ B-binding oligonucleotides and analysis of the electrophoretic retardation of protein-bound oligonucleotides revealed a comparable binding activity for both wild type and GFP-p65. The binding was specific for NF- κ B in both cases as shown by competition with a 200-fold molar excess of unlabeled oligonucleotides and the inability of a mutant competitor to prevent binding (Fig. 1). These results indicate that GFP-p65 binds *in vitro* to the NF- κ B cognate sequence as well as wild type p65 does. Our next goal was to verify whether GFP-NF- κ B fusion

proteins are also functional *in vivo*. For that purpose, we used reporter gene assays with a NF- κ B-dependent luciferase reporter. Transfection of HeLa cells with fusion proteins of p65 with GFP variants (GFP or YFP) induced a strong up-regulation of luciferase reporter activity, which reached the same level as with wild type p65 (Fig. 2). The induction of luciferase activity could be blocked both for wild type p65 and for GFP- or YFP-p65 by co-transfection of a vector coding for I κ B α , indicating that GFP-p65 variants are still binding *in vivo* to their physiologic inhibitor. Moreover, the same inhibition of NF- κ B-dependent reporter induction could be achieved by expressing a fusion protein of I κ B α with CFP linked to either the N or C terminus, demonstrating that GFP-p65 or YFP-p65 still bind to a I κ B α -GFP fusion protein. Similar results were obtained with 293 and CHO cells (data not shown). Taken together, these data indicate that GFP-p65 proteins are fully functional both *in vitro* and *in vivo*.

Fluorescence microscopy of different cell types (CHO, 293, HUVEC, and HeLa cells) that were transiently transfected with GFP-p65 revealed localization patterns dependent on the amount of protein expressed (Fig. 3A). Cells with low fluorescence intensity showed mainly cytosolic localization of the GFP-NF- κ B fusion protein, indicating complete binding to endogenous I κ B molecules. However, cells with a high expression level of GFP-p65 exhibited a predominant nuclear fluorescence, implying that the endogenous I κ B was saturated, leading to the nuclear translocation of the excess GFP-p65. Co-transfection of a YFP-p65 construct with a vector coding for CFP-I κ B resulted in cytosolic localization of both proteins in nearly all of the transfected cells, as demonstrated by microscopy filter combinations that distinguish between the two GFP variants. This observation supports the data obtained with reporter gene assays showing inhibition of NF- κ B activity by CFP-I κ B fusion proteins. Interestingly, transfection of CFP-I κ B without p65 revealed a predominant nuclear localization of the CFP-I κ B fusion protein. This fusion protein has a significantly higher molecular weight than the postulated limit for passive diffusion through the nuclear pore complex, indicating an active nuclear import, as previously demonstrated for the wild type I κ B (37, 38).

The interaction between YFP-p65 and CFP-tagged fusion proteins of I κ B α in the cytosol of living cells was further supported by FRET microscopy using ratio imaging of donor and acceptor fluorescence. This imaging technique revealed a significantly higher ratio of acceptor to donor fluorescence at the excitation wavelength of the donor for cells transfected with CFP-I κ B and YFP-p65 compared with control cells transfected with CFP and YFP investigated under the same conditions of transfection and imaging. Co-transfection of YFP-p65 with an I κ B-CFP construct, coding for a fusion protein with the CFP tag linked to the C terminus, where it should be closer to the YFP portion of p65 based on the known crystal structure (4, 5), revealed an even higher ratio of acceptor to donor fluorescence. The ratio image indicated YFP-p65-I κ B-CFP complexes in the cytosol, whereas that from the CFP/YFP control showed no remaining fluorescence signal (Fig. 3B). In addition to ratio imaging on a single cell level, we quantified the levels of fluorescence for a larger number of cells with donor and FRET filter sets in order to obtain average values, which should eliminate cell to cell variations of donor and acceptor expression. This quantitative evaluation showed a significantly increased ratio of acceptor to donor emission at the donor excitation wavelength and supported the FRET imaging results (data not shown).

We further verified the functional integrity of GFP-p65 by morphological analysis of transfected endothelial cells after

FIG. 2. Fusion proteins of p65 or I κ B α with GFP variants are functional in reporter gene assays. HeLa cells were transiently transfected in triplicates with a luciferase reporter construct containing a NF- κ B-dependent promoter (0.5 μ g/6-well plate), a plasmid coding for β -galactosidase under the control of a ubiquitin promoter (NF- κ B-independent) as internal control (0.5 μ g), and p65, I κ B α , or GFP variants thereof, as indicated (0.05 μ g of the p65 construct and 0.45 μ g of the I κ B α vector or an empty control vector). Cell extracts were prepared and luciferase as well as β -galactosidase activity determined as described under "Materials and Methods." Luciferase activity normalized to β -galactosidase is expressed as a -fold induction of control.

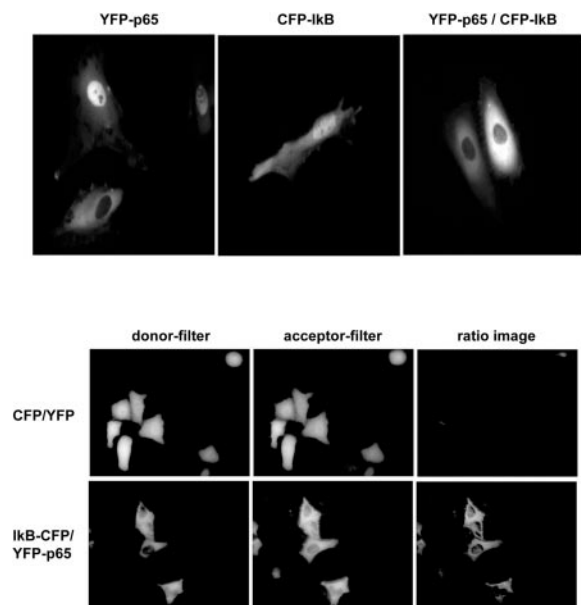
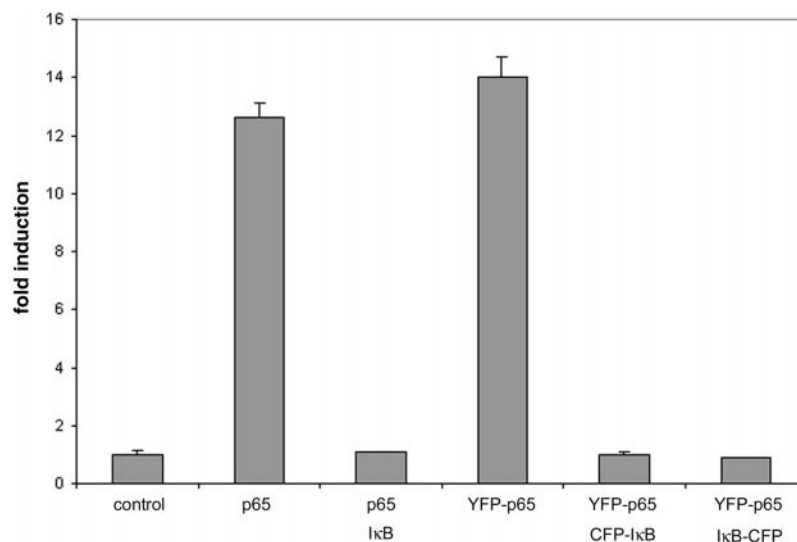


FIG. 3. Microscopy of YFP-p65 and CFP-I κ B α in living cells. *A*, HUVEC were transfected with YFP-p65 (*left panel*), CFP-I κ B α (*middle panel*), or both (*right panel*). Images were taken with a cooled CCD camera 1 day after transfection using the appropriate filter sets for CFP and YFP, respectively. The image in the *right panel* showed the same fluorescence pattern with both filter sets. *B*, FRET microscopy using ratio imaging. HeLa cells were transfected with equal amounts of CFP and YFP or I κ B-CFP and YFP-p65, and images were taken with the donor filter set and the acceptor filter set as described under "Materials and Methods." The ratio images represent the division of the acceptor filter images by the donor filter images. In the case of the negative control, fluorescence is higher with the donor filter set, whereas for the I κ B-CFP-YFP-p65 pair, it is higher in the acceptor filter set, resulting in a distinct ratio image.

administration of TNF α . Cells with a low expression level of GFP-p65 and a cytosolic localization, which reflect a physiological expression and regulation of the NF- κ B fusion protein, showed a marked translocation of GFP-p65 into the nucleus after TNF α administration (Fig. 4), indicating degradation of the endogenous I κ B and release of GFP-p65. Further investigation of GFP-p65 by fluorescence microscopy revealed subsequent nuclear export, which could be inhibited by leptomycin B, a drug that blocks nuclear export processes via exportin/ *crm1p* (data not shown). This finding is in line with previous reports demonstrating nuclear export of p65 bound to its in-

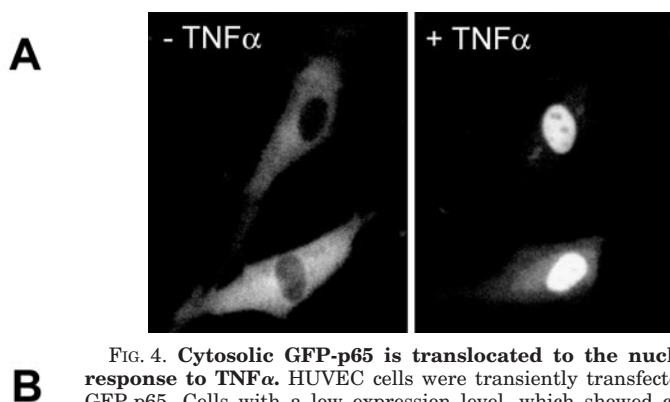


FIG. 4. Cytosolic GFP-p65 is translocated to the nucleus in response to TNF α . HUVEC cells were transiently transfected with GFP-p65. Cells with a low expression level, which showed cytosolic fluorescence, were investigated by confocal laser scanning microscopy followed by the addition of TNF α (200 u/ml) and subsequent morphological analysis of the same cells.

hibitor I κ B via a leptomycin B-sensitive, *crm1p*-dependent transport (37, 38).

Fluorescence Resonance Energy Transfer between GFP-NF- κ B and Fluorescently Labeled Oligonucleotides—After verifying the functional integrity of GFP-p65, we proposed to exploit the fluorescence properties of the fusion protein for studies on binding to its cognate DNA sequence by applying the principle of fluorescence resonance energy transfer (FRET). The fluorescence characteristics of enhanced GFP, with an excitation peak at 488 nm and the maximum emission at 507 nm, suggested the use of acceptor fluorophores with excitation peaks in the range of 500 to 540 nm. Commercially available covalent tags for oligonucleotides in that range are TET (tetrachloro-carboxyfluorescein) and HEX (hexachloro-carboxyfluorescein) with excitation peaks at 522 and 535 nm, respectively. Incubation of GFP-p65 extracts with TET-labeled NF- κ B-binding oligonucleotides showed a significant increase of acceptor fluorescence (Fig. 5A), detected as a distinct shoulder on the emission scan (after subtraction of the TET emission curve). The addition of increasing amounts of TET-labeled DNA to the GFP-p65 extract showed saturation characteristics of the FRET effect calculated as ratio of acceptor to donor fluorescence at the excitation wavelength of the donor (Fig. 5B).

Using HEX-labeled DNA as the acceptor, we observed only a slight increase in acceptor fluorescence but a significant decrease in GFP emission. This decrease was a DNA sequence-specific effect as shown by the restoration of the donor fluores-

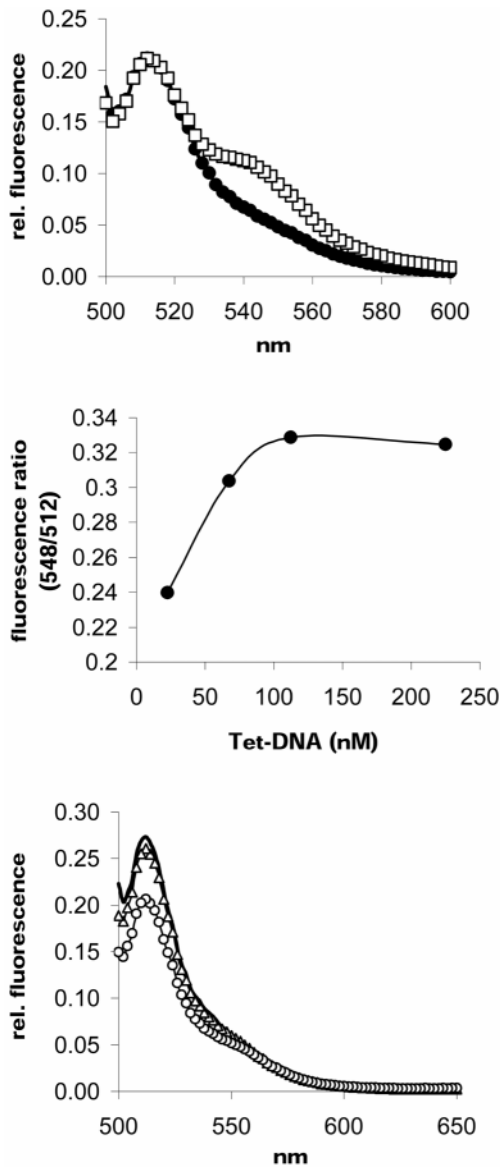


FIG. 5. Binding between GFP-p65 and fluorescently labeled oligonucleotides can be monitored by FRET analysis. *A*, extracts from stable CHO transfectants expressing GFP-p65 were incubated with TET-labeled NF- κ B-binding oligonucleotides (in the presence of 0.1 mg/ml poly(dI-dC)) and analyzed by scanning fluorometry with excitation of the donor fluorophore, GFP. The emission curve of the TET fluorescence in the absence of GFP-p65 was subtracted from the emission scan of the sample containing both fluorophores. The resulting emission curve (GFP-p65-Tet-DNA, \square) was compared with the GFP-p65 emission in the absence of labeled oligonucleotides (GFP-p65, \bullet). *B*, equal amounts of GFP-p65 extracts were incubated with increasing amounts of TET-labeled oligonucleotides and measured by fluorometry. FRET was determined by calculating the ratio of acceptor fluorescence to donor fluorescence. This ratio is plotted against the concentration of oligonucleotide. *C*, FRET between GFP-p65 and HEX-labeled oligonucleotides (determined as in *A*) shows a significant decrease of donor fluorescence (GFP-p65-Hex-DNA, \circ) compared with GFP-p65 alone (thick line). The addition of an unlabeled competitor oligonucleotide in excess restores the donor emission (\triangle)

cence after the addition of unlabeled competitor DNA in excess (Fig. 5C). We assume that the rather small overlap of the GFP emission with the excitation spectrum of HEX favors a donor quenching rather than an increase in acceptor fluorescence.

Kinetics of GFP-NF- κ B Binding to DNA—The application of the FRET principle allowed us to obtain much more information on the binding process between proteins and DNA than would the use of conventional techniques such as electro-

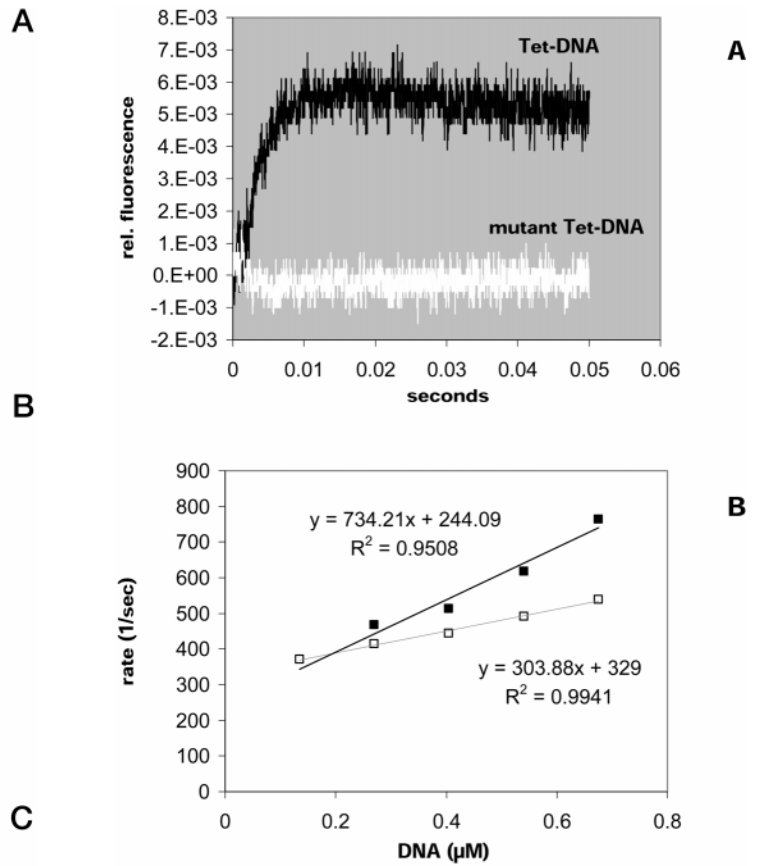


FIG. 6. Kinetics of binding between GFP-p65 and fluorescently labeled DNA as measured by stopped-flow fluorometry of the FRET. *A*, GFP-p65 extracts were mixed with TET-labeled NF- κ B-binding oligonucleotides (*Tet-DNA*) or labeled nonbinding oligonucleotides (*mutant Tet-DNA*) at 15 °C in the mixing chamber of a stopped-flow system, and the acceptor fluorescence at the excitation of the donor was recorded for 50 ms. *B*, equal amounts of GFP-p65 extracts were mixed with increasing concentrations of TET-labeled NF- κ B-binding oligonucleotides and the kinetics of binding measured by stopped-flow fluorometry for 50 ms. The resulting time course of the acceptor fluorescence was fitted by a single exponential algorithm to obtain the initial binding rates. The observed rates for 37 °C (\blacksquare) and 15 °C (\square) are plotted against the concentration of the oligonucleotide, and the corresponding correlation is calculated by linear regression. The *y* axis intercept indicates the off-rate, and the slope of the line is a measure for the on-rate of binding.

phoretic mobility shift assays. One of the advantages is the possibility of determining the kinetics of the association by monitoring the time course of the FRET effect. We aimed to determine the kinetics of GFP-NF- κ B binding to DNA by using stopped-flow fluorometry, which is suited to the measurement of changes in fluorescence in the millisecond range. Mixing a cell extract from stable transfectants expressing GFP-p65 with a TET-labeled NF- κ B-binding oligonucleotide resulted in a distinct increase of acceptor fluorescence at the donor excitation wavelength, reaching a plateau as soon as about 10 ms (Fig. 6A). No temporal change of fluorescence was observed with a mutant TET-labeled DNA sequence that does not bind to NF- κ B.

For a further evaluation of the binding process, we investigated the concentration dependence of the observed initial binding rates at 15 and 37 °C deduced from single exponential fits between 1 and 10 ms (Fig. 6B). Interestingly, we found rather high off-rates of $3.3 \times 10^2 \text{ s}^{-1}$ and $2.4 \times 10^2 \text{ s}^{-1}$ for 15 and 37 °C, respectively. Given the on-rates, deduced from Fig. 6B, of $3.0 \times 10^8 \text{ M}^{-1} \text{ s}^{-1}$ and $7.3 \times 10^8 \text{ M}^{-1} \text{ s}^{-1}$, we calculate association constants K_d $9.2 \times 10^5 \text{ M}^{-1}$ and $3.0 \times 10^6 \text{ M}^{-1}$ for 15

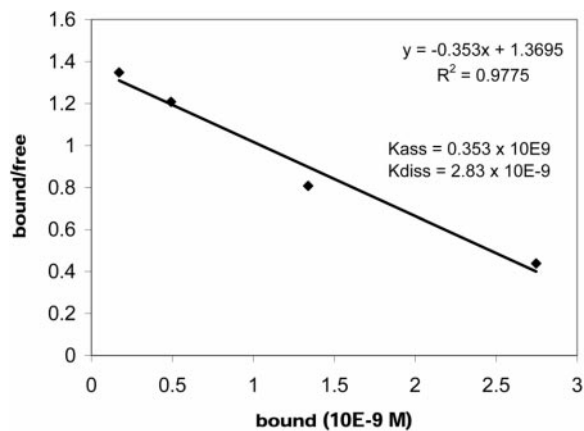


FIG. 7. Affinity of GFP-p65 for NF- κ B-binding oligonucleotides as determined by an equilibrium binding assay (electrophoretic mobility shift assay). Constant amounts GFP-p65 extracts were incubated for 15 min with different concentrations of 32 P-labeled NF- κ B-binding oligonucleotides and subjected to native polyacrylamide gel electrophoresis. NF- κ B-bound and free radioactivity were quantified using a PhosphorImager and analyzed by Scatchard plotting. The equation and the correlation coefficient of the linear regression fit are given, as well as the deduced association and dissociation constants.

and 37 °C, respectively. These constants are significantly lower than postulated in previous reports, which claim association constants in the range of 10^{10} M^{-1} for p65 homodimers as determined by electrophoretic mobility shift assays done by Fujita *et al.* (19).

To clarify whether this difference in the calculated binding affinity from previously reported values is due to a reduced affinity of the GFP fusion protein or a difference in pre-steady state *versus* equilibrium binding affinity, we applied the same technique of electrophoretic mobility shift titration assays that was previously used to determine the equilibrium binding constants. Constant amounts of GFP-NF- κ B extracts were incubated with increasing amounts of radioactively labeled NF- κ B-binding oligonucleotides and subjected to gel electrophoresis. The relation of bound to free oligonucleotides was used to calculate the association constant by Scatchard analysis, revealing a value of about $4 \times 10^8 \text{ M}^{-1}$ (Fig. 7). This number is somewhat lower than that reported for p65 homodimers but is still significantly higher than that calculated from off- and on-rates determined by stopped-flow analysis. These data indicate that the GFP portion of the fusion protein may cause some reduction in the equilibrium binding affinity. However, it is apparently not the reason for the distinct difference between the affinity determined by analysis of the pre-steady state kinetics and that observed under equilibrium conditions. One possibility would be that a second, slower reaction takes place, which increases the overall affinity. To test for this possibility, we investigated the FRET effect between GFP-p65 and TET-labeled oligonucleotides for longer time periods. These studies showed a rather slow decrease of FRET, which became noticeable after about 20 ms (Fig. 8A). This decrease was more noticeable at 37 °C with approximately 30% reduction of the FRET effect between 10 and 50 ms, whereas it was only about 10% in the same time at 15 °C (Fig. 6A). The decline was not due to a bleaching process, because GFP-p65 or TET-labeled oligonucleotide alone showed no reduction of fluorescence (data not shown). This second phase of the interaction between GFP-p65 and oligonucleotides could be fitted by a decay of fluorescence with the natural logarithm of time according to the formula: fluorescence = $k \times \ln(\text{time})$. Analysis of the second phase with different amounts of oligonucleotides could not detect any significant correlation between the constant k and the oligonucleotide concentration (Fig. 8B). In principle, a dissoci-

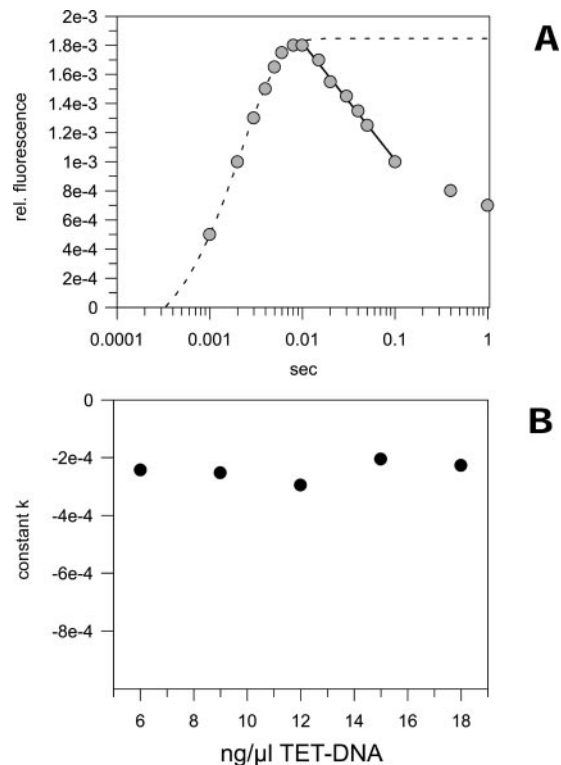


FIG. 8. Stopped-flow analysis of the FRET effect indicates a conformational transition of the GFP-p65-TET-DNA complex after the binding. **A**, kinetics of the FRET effect on a logarithmic time scale. The interaction between GFP-p65 and TET-labeled oligonucleotides was measured at 37 °C by stopped-flow fluorimetry with 2000 data sets for the initial 50 ms and 2000 data points for the subsequent 1000 ms. Representative points are shown and fitted by a single exponential equation (dashed line) between 1 and 10 ms and by a logarithmic algorithm (fluorescence = $k \times \ln(\text{time})$, solid line) between 10 and 100 ms. The absolute fluorescence of the GFP-p65 extract was lower than that used in Fig. 6A, resulting in a lower absolute amplitude of the fluorescence change. **B**, equal amounts of GFP-p65 were analyzed with increasing concentrations of TET-labeled oligonucleotides, and the second phase of the interaction (10–100 ms) was fitted with the logarithmic algorithm. The calculated constant, k , is plotted against the oligonucleotide concentration, indicating no concentration dependence of the second phase.

ation of GFP-NF- κ B and the TET-labeled oligonucleotide could be a potential reason for the observed decrease of the FRET. However, in that case there should be a linear correlation between the natural logarithm of the fluorescence and time (39). Moreover, electrophoretic mobility shift assays indicated a strong, high affinity binding of the oligonucleotide to GFP-p65 even after prolonged incubation. Therefore, we assume that the observed decrease of fluorescence is caused by a conformational change of the GFP-p65-DNA complex.

DISCUSSION

We generated a fusion protein of p65 NF- κ B with enhanced GFP on the N terminus and demonstrated the functional integrity of this chimeric protein both *in vitro* and *in vivo* by the use of electrophoretic mobility shift and reporter gene assays, respectively. Under normal conditions of gel retardation assays, where an excess of oligonucleotides is used, we observed binding of GFP-p65 to its cognate DNA motif that was equivalent to that of wild type p65. However, this observation does not rule out the possibility that the affinity is lower under nonsaturating conditions. In fact, electrophoretic mobility shift assays with various nonsaturating concentrations of NF- κ B-binding oligonucleotides suggested a slightly lower affinity of GFP-p65 compared with values reported for wild type p65 (19),

which might be the result of the GFP moiety. Furthermore, the difference between reported affinities and those that we found in electrophoretic mobility shift assays might have been caused by subtle differences in the oligonucleotide sequence. Nonetheless, using reporter gene assays, we found an equivalent activity *in vivo* of GFP-p65 and wild type p65 with respect to the induction of NF- κ B-dependent promoters. Moreover, the GFP fusion protein was inhibited by I κ B, as is wild type p65, and could also be blocked by a fusion protein of I κ B and CFP, demonstrating that the transcription factor can bind *in vivo* to its physiologic inhibitor even when both proteins are linked to a GFP variant. These findings were further supported by FRET microscopy, using ratio imaging of donor and acceptor fluorescence, and by morphological analysis, showing that CFP-I κ B and YFP-p65 prevent each other from translocating into the nucleus.

Transient overexpression of GFP-p65 without its inhibitory molecule I κ B led to a distinct fluorescence localization pattern depending on the expression level. Although cells with rather low fluorescence exhibited a cytosolic localization of GFP-NF- κ B, cells with a high expression level showed a predominant nuclear fluorescence. We assume that the cytosolic localization of GFP-p65 in cells with low expression is due to binding to endogenous I κ B rather than to a putative nuclear export sequence recently postulated to be active in COS cells (40). This notion was supported by the observation that TNF α induced a nuclear translocation of cytosolic GFP-p65, which can be explained by a degradation of bound endogenous I κ B, whereas it is unlikely to affect a putative nuclear export mechanism of p65. Moreover, transfection experiments using low amounts of the GFP-p65 vector revealed a predominant cytosolic fluorescence, whereas co-expression of the same amount of GFP-p65 with an excess of unlabeled p65 lead to a significant shift from cytosolic to nuclear fluorescence, indicating that the endogenous I κ B is saturated by the unlabeled p65 (data not shown). It might be dependent on the cell type as to whether the localization of p65 is regulated by I κ B molecules or by an intrinsic nuclear export sequence. This view is supported by the observation that overexpression of p65 leads to a predominant cytosolic localization in COS cells (40), whereas the majority of endothelial cells exhibit a nuclear localization.

Our results on nuclear translocation of cytosolic GFP-p65 after the addition of TNF α to transfected HUVEC is also in line with a very recent report showing the nuclear import of a GFP-p65 fusion protein in fibroblasts in response to interleukin 1 β (41).

The localization that we observed for CFP-I κ B in the absence of co-transfected p65 is further support for the current assumption that I κ B is actively transported into the nucleus instead of undergoing a passive diffusion as formerly suggested (42, 43). The fusion protein is significantly larger than the threshold value for diffusion through the pore complex, whereas wild type I κ B would be small enough for such a passive translocation. In a recent report, it has been demonstrated that there is an active nuclear import of I κ B *in vitro*, which requires the ankyrin repeats (44). However, the quantitative relation of this active transport compared with a potential passive diffusion is not known in detail for the *in vivo* situation. Our results imply that the active nuclear import might constitute the major portion of the transport or is at least capable of transferring nearly all of the I κ B α , because we find *in vivo* a predominant nuclear fluorescence after overexpression of CFP-I κ B. After verifying the functional integrity of GFP-p65 in various assays, we aimed to exploit its fluorescence properties for binding studies with fluorescently labeled DNA using FRET technology. We were able to monitor a significant change of the emission curve with

different fluorophores that we used as labels for the NF- κ B-binding oligonucleotides. Incubation of GFP-p65 with TET-labeled oligonucleotides resulted in a significant increase in acceptor fluorescence, whereas incubation with HEX-labeled DNA caused rather a decrease of donor and only a slight augmentation of acceptor fluorescence. The observed difference between TET- and HEX-labeled oligonucleotides in energy transfer experiments with GFP-p65 might result from the smaller overlap between the emission spectrum of GFP and the excitation spectrum of HEX compared with that of TET, which would favor a consumption of the absorbed energy by other mechanisms, such as molecular oscillations, instead of emission of acceptor fluorescence. However, for both fluorophores the detected spectral shifts were DNA sequence-specific, as shown by competition experiments or labeled oligonucleotides that do not bind to NF- κ B. Our data on the kinetics of the binding process between NF- κ B and DNA, using stopped-flow fluorometry of the FRET effect between GFP-p65 and TET-labeled oligonucleotides, provide important information for the dynamics of this transcription factor. In principle, stopped-flow measurements of binding reactions can be achieved, at least in certain cases, by monitoring changes of the intrinsic tryptophan fluorescence caused by conformational changes. However, the application of functional GFP fusion proteins and FRET analysis seems especially useful in stopped-flow measurements because it circumvents the need for highly purified protein preparations, which are normally necessary for the determination of intrinsic fluorescence and which often retain only part of the original physiologic activity.

Using time-resolved FRET analysis, we showed that the association between GFP-p65 and the corresponding oligonucleotides occurs within several ms. The first reports using equilibrium binding studies based on electrophoretic mobility shift assays proposed a very slow binding process with a plateau after about 60 min (21), which seems rather unlikely given the high affinity of this transcription factor for its cognate DNA sequence, which has an association constant in the range of 10^{10} to 10^{12} M $^{-1}$ (19). It has to be noted that the binding reaction in the study of Zabel and Baeuerle (21) was done in the presence of 100 μ g/ml poly(dI-dC), which is usually added in electrophoretic mobility shift assays to improve the specificity of the technique. However, later studies of the same group demonstrated that this compound has to be omitted in experiments measuring the affinity of binding, because it is a significant competitor of the binding process with an IC $_{50}$ concentration of about 38 μ g/ml and also influences the kinetics of association. Gel retardation assays in the absence of poly(dI-dC) revealed an equilibrium of the binding process within less than 5 min (22), which is apparently faster than the time limit that can be resolved by that technique. Our present study is, to our knowledge, the first report on the kinetics of binding between a NF- κ B molecule and its cognate DNA sequence in solution using a technique that is suited to resolve reactions in the millisecond range. Interestingly, the affinity that we calculated based on k_{on} and k_{off} rates derived from pre-steady state kinetics is significantly lower than the value derived from Scatchard analysis of data obtained by electrophoretic mobility shift assays using the same GFP-p65 preparation. Although we found somewhat lower steady state affinities for the GFP-p65 fusion protein compared with values reported for wild type p65 homodimers (19), the GFP moiety is apparently not the reason for the observed difference between the association constant calculated from pre-steady state kinetics and that derived from equilibrium binding studies. A possible explanation for this difference is that the binding process includes a fast association with lower affinity, which is

followed by a slower reconfiguration of the complex leading to an increase of the association constant. Stopped-flow analysis of the FRET effect for 1 s actually indicated a conformational transition after the first binding process, resulting in a decrease of FRET. This decrease was not due to bleaching of fluorophores and it could not be explained by dissociation of GFP-p65 and TET-labeled DNA, because it did not follow the kinetics of a dissociation process. Moreover, electrophoretic mobility shift assays, which were done after 15 min of incubation, still showed a strong, high affinity binding. The observed decrease of fluorescence might be caused by an increased distance between the GFP tag and the TET label or, alternatively, by a decrease of the distance between the two GFP molecules of a GFP-p65 homodimer, resulting in a mutual donor quenching and a subsequent decrease of acceptor fluorescence. The on-rate that we measured for the first stage of binding between GFP-p65 and DNA is comparable with or even higher than values reported for other DNA-binding proteins. However, the off-rate of $2.4 \times 10^2 \text{ s}^{-1}$ that we observed for this initial phase seems considerably higher than the off-rates reported for these proteins (34, 45, 46). It is possible that a subsequent decrease of the off-rate due to a conformational change results in a corresponding increase of the association constant. A decrease of k_{off} to a number in the range of 10^0 s^{-1} , as described for RNA polymerase (34), would lead to a corresponding increase of the association constant from $3 \times 10^6 \text{ M}^{-1}$ to $10^8\text{-}10^9 \text{ M}^{-1}$, which would be in line with our data obtained from equilibrium binding assays.

It has to be noted, however, that these values derived from *in vitro* studies cannot reflect the complexity of the situation *in vivo*, where the conditions for diffusion and accessibility of NF- κ B binding sequences are probably significantly different.

Nevertheless, our study demonstrates that GFP fusion proteins are not only useful in investigating the dynamics of a great variety of proteins in living cells but also in monitoring the biochemical characteristics of macromolecular interactions in solution by means of time-resolved measurements of FRET in the millisecond range. The application of this technique to the investigation of protein-protein interactions using appropriate GFP variants might expand our understanding of these interactions considerably.

Acknowledgments—The expert technical assistance of Michaela Kind is gratefully acknowledged. We thank Christine Brostjan and Roger Sleight for carefully reading the manuscript and our colleagues from the Vienna International Research Cooperation Center for stimulating discussions and continuous support.

REFERENCES

- Siebenlist, U., Franzoso, G., and Brown, K. (1994) *Annu. Rev. Cell Biol.* **10**, 405–455
- Baldwin, A. S., Jr. (1996) *Annu. Rev. Immunol.* **14**, 649–683
- de Martin, R., Schmid, J. A., and Hofer-Warbinek, R. (1999) *Mutat. Res.* **437**, 231–243
- Huxford, T., Huang, D. B., Malek, S., and Ghosh, G. (1998) *Cell* **95**, 759–770
- Jacobs, M. D., and Harrison, S. C. (1998) *Cell* **95**, 749–758
- Mercurio, F., and Manning, A. M. (1999) *Curr. Opin. Cell Biol.* **11**, 226–232
- Vandenabeele, P., Declercq, W., Beyaert, R., and Fiers, W. (1995) *Trends Cell Biol.* **5**, 392–399
- Malinin, N. L., Boldin, M. P., Kovalenko, A. V., and Wallach, D. (1997) *Nature* **385**, 540–544
- Nakano, H., Shindo, M., Sakon, S., Nishinaka, S., Mihara, M., Yagita, H., and Okumura, K. (1998) *Proc. Natl. Acad. Sci. U. S. A.* **95**, 3537–3542
- Nemoto, S., DiDonato, J. A., and Lin, A. (1998) *Mol. Cell. Biol.* **18**, 7336–7343
- DiDonato, J. A., Hayakawa, M., Rothwarf, D. M., Zandi, E., and Karin, M. (1997) *Nature* **388**, 548–554
- Regnier, C. H., Song, H. Y., Gao, X., Goeddel, D. V., Cao, Z., and Rothe, M. (1997) *Cell* **90**, 373–383
- Zandi, E., Rothwarf, D. M., Delhase, M., Hayakawa, M., and Karin, M. (1997) *Cell* **91**, 243–252
- Mercurio, F., Zhu, H., Murray, B. W., Shevchenko, A., Bennett, B. L., Li, J., Young, D. B., Barbosa, M., Mann, M., Manning, A., and Rao, A. (1997) *Science* **278**, 860–866
- Woronicz, J. D., Gao, X., Cao, Z., Rothe, M., and Goeddel, D. V. (1997) *Science* **278**, 866–869
- Spencer, E., Jiang, J., and Chen, Z. J. (1999) *Genes Dev.* **13**, 284–294
- Yaron, A., Hatzubai, A., Davis, M., Lavon, I., Amit, S., Manning, A. M., Andersen, J. S., Mann, M., Mercurio, F., and Ben-Neriah, Y. (1998) *Nature* **396**, 590–594
- Whiteside, S. T., Epinat, J. C., Rice, N. R., and Israel, A. (1997) *EMBO J.* **16**, 1413–1426
- Fujita, T., Nolan, G. P., Ghosh, S., and Baltimore, D. (1992) *Genes Dev.* **6**, 775–787
- Chen, Y. Q., Ghosh, S., and Ghosh, G. (1998) *Nat. Struct. Biol.* **5**, 67–73
- Zabel, U., and Baeuerle, P. A. (1990) *Cell* **61**, 255–265
- Zabel, U., Schreck, R., and Baeuerle, P. A. (1991) *J. Biol. Chem.* **266**, 252–260
- Urban, M. B., and Baeuerle, P. A. (1990) *Genes Dev.* **4**, 1975–1984
- de la Torre, A., Schroeder, R. A., and Kuo, P. C. (1997) *Biochem. Biophys. Res. Commun.* **238**, 703–706
- Herman, B. (1989) *Methods Cell Biol.* **30**, 219–243
- Clegg, R. M. (1995) *Curr. Opin. Biotechnol.* **6**, 103–110
- Szollasi, J., Damjanovich, S., and Matyus, L. (1998) *Cytometry* **34**, 159–179
- de Martin, R., Vanhove, B., Cheng, Q., Hofer, E., Csizmadia, V., Winkler, H., and Bach, F. H. (1993) *EMBO J.* **12**, 2773–2779
- Stehlik, C., de Martin, R., Kumabashiri, I., Schmid, J. A., Binder, B. R., and Lipp, J. (1998) *J. Exp. Med.* **188**, 211–216
- Wrighton, C. J., Hofer-Warbinek, R., Moll, T., Eytner, R., Bach, F. H., and de Martin, R. (1996) *J. Exp. Med.* **183**, 1013–1022
- Ruben, S. M., Dillon, P. J., Schreck, R., Henkel, T., Chen, C. H., Maher, M., Baeuerle, P. A., and Rosen, C. A. (1991) *Science* **251**, 1490–1493
- de Wet, J. R., Wood, K. V., De Luca, M., Helinski, D. R., and Subramani, S. (1987) *Mol. Cell. Biol.* **7**, 725–737
- Periasamy, A., and Day, R. N. (1999) *Methods Cell Biol.* **58**, 293–314
- Johnson, R. S., and Chester, R. E. (1998) *J. Mol. Biol.* **283**, 353–370
- Chen, F. E., Huang, D. B., Chen, Y. Q., and Ghosh, G. (1998) *Nature* **391**, 410–413
- Wang, D., and Baldwin, A. S., Jr. (1998) *J. Biol. Chem.* **273**, 29411–29416
- Arenzana-Seisdedos, F., Turpin, P., Rodriguez, M., Thomas, D., Hay, R. T., Virelizier, J. L., and Dargemont, C. (1997) *J. Cell Sci.* **110**, 369–378
- Johnson, C., Van Antwerp, D., and Hope, T. J. (1999) *EMBO J.* **18**, 6682–6693
- Lu, T., and Sawadogo, M. (1994) *J. Biol. Chem.* **269**, 30694–30700
- Harhaj, E. W., and Sun, S. C. (1999) *Mol. Cell. Biol.* **19**, 7088–7095
- Carlotti, F., Chapman, R., Dower, S. K., and Qwarnstrom, E. E. (1999) *J. Biol. Chem.* **274**, 37941–37949
- Zabel, U., Henkel, T., Silva, M. S., and Baeuerle, P. A. (1993) *EMBO J.* **12**, 201–211
- Cressman, D. E., and Taub, R. (1993) *Oncogene* **8**, 2567–2573
- Turpin, P., Hay, R. T., and Dargemont, C. (1999) *J. Biol. Chem.* **274**, 6804–6812
- Perez-Howard, G. M., Weil, P. A., and Beechem, J. M. (1995) *Biochemistry* **34**, 8005–8017
- van Leeuwen, H. C., Strating, M. J., Rensen, M., de Laat, W., and van der Vliet, P. C. (1997) *EMBO J.* **16**, 2043–2053